

ELECTRON BEAMS FROM 10^{11} - 10^{12} WATT PULSED ACCELERATORS

by W. T. Link

Physics International Company
San Leandro, California

I. Introduction

Recently developed pulsed power systems are capable of producing pulsed relativistic electron beam currents in the 10^5 -ampere range. The behavior of these electron beams is completely dominated by their large self-created electric and magnetic fields. This paper describes current research on the behavior of these intense electron beams.

II. Description of Accelerators

Figure 1 shows the basic components of the pulsed accelerators used at Physics International Company to accelerate 10^5 -ampere electron beams.

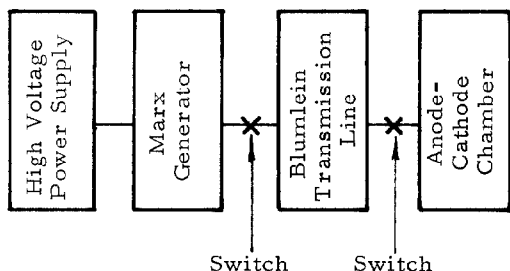


Figure 1. Block Diagram of Pulsed Electron Accelerator

The components include a standard high-voltage charging supply, a Marx voltage generator (parallel charge, series discharge of capacitors), a resonance-charged Blumlein transmission line, and a cathode-anode region across which electrons are accelerated. The cathode-anode region is at high vacuum and all the remaining parts of the machine are submerged in insulating oil. Most of the descriptive matter of this paper will apply to the Physics International Company Model 730 electron accelerator.

Figure 2 is a schematic diagram of the cathode-anode chamber and the electron-beam chamber. The Blumlein line delivers a 5-MV, 30×10^{-9} -second negative pulse to the cathode. The electric field at the cathode tip ($\sim 10^8$ V/cm) is then sufficient to cause direct field emission of electrons from the cathode toward the anode. The magnitude of electron current and the kinetic energy of the electrons are governed by the Blumlein characteristic impedance ($\sim 50 \Omega$) and by the equivalent impedance of the cathode-anode

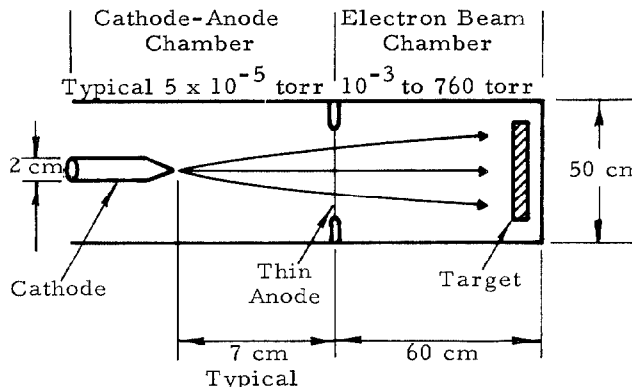


Figure 2. Arrangement of Anode-Cathode and Electron-Beam Chambers

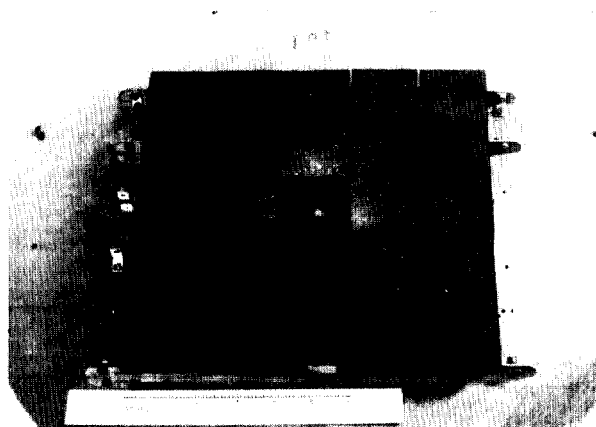
space ($\sim 50 \Omega$), and are typically 50,000 amperes and 3 MeV respectively. The stream of electrons strikes the thin anode and passes out into the electron-beam chamber.

In summary, we have available in the electron-beam chamber a 50,000 ampere, 30×10^{-9} -second-long burst of 3-MeV electrons with a cross sectional area at the anode of about 10 cm^2 .

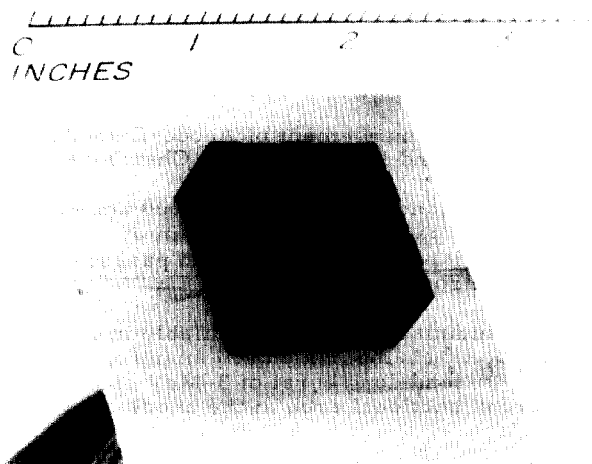
III. Diagnostic Equipment

The design of electron-beam diagnostic equipment is governed by the fact that most material objects placed in the path of the beam are destroyed by a single burst of electrons. Further limitations are the high noise levels in the vicinity of the machine (tens of volts) and the necessary use of gas in the electron chamber (see below), which severely limits the usefulness of Faraday cups and magnetic and electric probes.

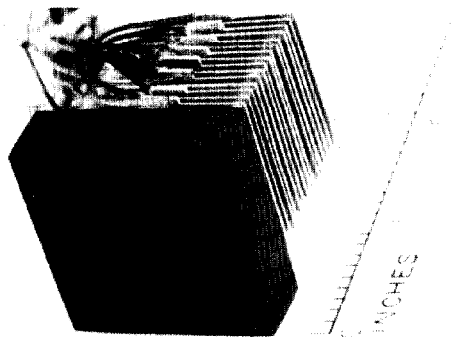
Calorimetry, using graphite blocks as beam stoppers, survives all of these limitations and is the most important diagnostic tool presently in use. Figure 3 shows several calorimeter types. Figures 3a and 3b show large and small graphite calorimeter arrays used to measure the electron-beam intensity as a function of distance from the beam-chamber centerline. Figure 3c shows a stack of aluminum disks used to determine the electron beam energy deposition as a function of the depth of penetration into the aluminum. The thermal equilibrium time in the various calorimeter blocks is on the order of one second and the cooling time is on the order of one minute, so



(a) Large Calorimeter Array for Measuring Radial Beam Intensity



(b) Small Calorimeter Array for Measuring Radial Beam Intensity



(c) Stack of Calorimeter Foils To Measure Energy Deposition with Depth of Electron Beams

Figure 3. Arrays of Calorimeters. Graphite withstands repeated electron beam shots. Aluminum is used only at very low electron-beam intensity.

that a thermocouple sampling switch that samples and digitally records at the rate of 20 thermocouples per second is adequate to provide good data from up to 50 calorimeter elements.

Photography, electric and magnetic probes, Faraday cups, X-ray dose measurement, and magnetic analysis are also used when appropriate.

IV. Behavior of Electron Beams as a Function of the Gas Pressure in the Beam Chamber

Figure 4 shows photographs of the electron beam traversing the beam chamber at various air pressures.

Much of the theory of electron streams is summarized in a general paper by Lawson (1959).¹

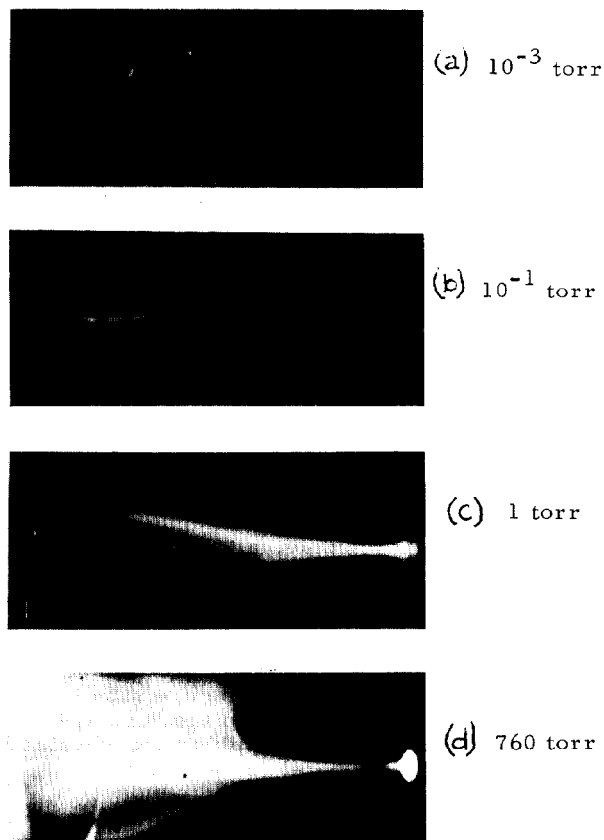


Figure 4. Behavior of 3-MeV, 50,000-Ampere Electron Beams in Air at Various Pressures. The beam chamber is 50 cm long and the camera is about 30 cm from the chamber centerline. The camera shutter is opened a second before and closed a second after the shot.

The electric, magnetic, and total forces on an electron at the surface of a cylindrical electron beam in a vacuum are

$$F_e = \frac{2Ne^2}{4\pi\epsilon_0 r} \quad (1)$$

$$F_m = \frac{-2Ne^2}{4\pi\epsilon_0 r} \beta^2 \quad (2)$$

$$F = F_e + F_m = \frac{2Ne^2}{4\pi\epsilon_0 r} [1 - \beta^2] \quad (3)$$

where F_e is the radially outward electric force (N)
 F_m is the radially inward magnetic force (N)
 $F = F_e + F_m$ is the total force (N)
 N is the number of electrons per meter
 r is the radius of the beam (m)
 $\beta = \frac{v}{c}$.

For 50,000 amperes and 3 MeV kinetic energy, the force is large and radially outward. As Figure 4a shows, the beam blows up and a remaining part of it fills the chamber roughly uniformly.

If the electron-beam chamber is filled with a low-pressure gas, the self-forces in the beam are greatly modified. The high-energy electrons ionize the gas, freeing secondary electrons that are then repelled by the large radial electric field. The remaining positive ions tend to electrically neutralize the electron beam; this is represented by multiplying Equation 1 by an electric neutralization factor f_e . Thus

$$F_e = \frac{2Ne^2}{4\pi\epsilon_0 r} f_e; \quad 0 < f_e < 1. \quad (4)$$

The rapid rise of magnetic field when the electron beam passes into the beam chamber produces a large voltage in the backward direction. This backward voltage may, at suitable pressure, produce a backward current that neutralizes or nearly neutralizes the magnetic field, and this is represented by multiplying Equation 2 by a magnetic neutralization factor f_m . Thus

$$F_m = \frac{-2Ne^2}{4\pi\epsilon_0 r} \beta^2 f_m; \quad 0 < f_m < 1. \quad (5)$$

The total force is then

$$F = \frac{2Ne^2}{4\pi\epsilon_0 r} [1 - f_e - \beta^2 (1 - f_m)] \quad (6)$$

Equation 6 assumes a steady-state condition, ignores possible cooperative phenomena in the beam, and ignores possibly large longitudinal forces.

The table below summarizes the conditions that can be seen in Figure 4. A continuum of intermediate conditions exists, but we shall deal here only with the four cases shown.

Fig.	Chamber Pressure (torr)	Observed Behavior of Beam	Likely Values of f_e, f_m	Force On Electron*
4a	10 ⁻³	Beam blows up.	$f_e = 0,$ $f_m = 0$	$1 - \beta^2 \approx 0.02$
4b	10 ⁻¹	Beam pinches a few mm diameter.	$f_e = 1,$ $f_m = 0$	$-\beta^2 \approx -1.0$
4c	1	Beam drifts with nearly zero force.	$f_e = 1,$ $f_m = 1$	0
4d	760	Beam pinches; multiple scattering in air finally breaks up pinch.	$f_e = 1,$ $f_m = 0$	$-\beta^2 \approx -1.0$

*This is the force on an electron at the surface of a beam divided by $\frac{2Ne^2}{4\pi\epsilon_0 r}$.

The values of f_e and f_m assumed in this table are consistent with order-of-magnitude calculations based on primary ionization by the beam, the build-up of large backward currents of low-energy electrons, and finally the suppression of these large backward currents (at high pressure) through the reduction of electron mean free path.

V. Image Forces in a Conductor

A pulsed electron beam develops a mirror image of itself in a conductor. The rapidly rising magnetic field associated with the beam produces eddy currents and magnetic fields in a conductor that appear to derive from an equal but opposite current equally spaced behind the conductor. Unneutralized charge in an electron beam produces a mirror image charge in the usual way.

The image force from a flat conductor on an electron of an electron beam parallel to the conductor is

$$F_{\text{image}} = \frac{-Ne^2}{4\pi\epsilon_0 r} \left[1 - f_e - \beta^2 (1 - f_m) \right] \quad (7)$$

where r is the distance of the beam from the conductor and all other symbols are as defined in Equations 3 and 6.

If the electron beam is pinched, f_e equals approximately 1, and the image force should be repulsive. Figure 5 is a side photograph of such a pinched beam. The drawing in Figure 5 shows why the beam reflects downward after leaving the conducting sheet; it simply "sees" the top of the beam chamber and reflects away from it. The

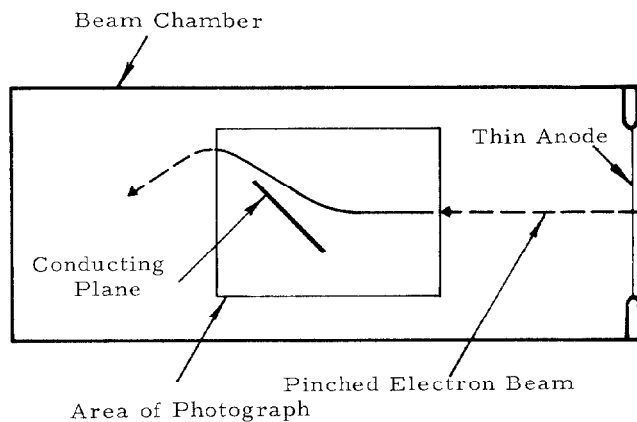
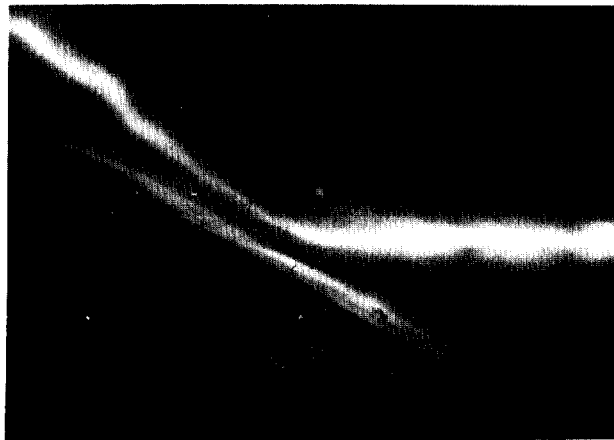


Figure 5. A Pinched Electron Beam Reflecting from a Conducting Sheet. The conducting sheet is grounded to the beam chamber. In four shots there was no damage of any sort to the conductor. Had the conducting sheet been normal to the beam a large hole in the sheet would have resulted from each shot.

differential equation that governs the motion of the beam in this case is

$$\frac{d^2 r}{dZ^2} - \frac{1}{I_0 \gamma} \frac{1}{r} = 0, \quad (8)$$

where I is the total current in the pinch.

$$I_0 = \frac{ec}{r_0} \approx 17,000 \text{ amperes}$$

$$\gamma = \frac{1}{\sqrt{1 - \beta^2}}$$

The solution of this equation,² when referred to Figure 5, indicates the beam current in Figure 5 is about 20,000 amperes, a reasonable result.

An electrically and magnetically neutralized beam should have no image force ($f_e \sim f_m \sim 1$ in Equation 7). Experimentally, it has been observed that such a beam shows little or no tendency to reflect from a conducting surface.

VI. Radial Cross Sections of Electron Beams

Pinched Beams, Figure 4b

One half to one third of the total beam draws down to a very small, intense pinch. Our smallest calorimeter array consists of twenty-five 0.5-cm-square blocks. The resolution of this array permits only a lower limit to be assigned for the peak current intensity: 20,000 ampere/cm² (500 calories/cm² for 3-MeV electrons in a 30×10^{-9} -second burst). The pinch is stable for at least the 50-cm length of the beam chamber and can be bent in a magnetic field with the same deflection as would occur for the individual 3-MeV electrons.

Drifting Beams, Figure 4c

In this mode the entire beam drifts from the anode to the end of the beam chamber with little indication of internal forces. The angular divergence of the electron beam is then 0.2 radians FWHM but this can be increased to any reasonable value by locating a thin scattering foil at the anode. The electron-beam intensity falls off roughly as the inverse square of the distance from the anode and is observed to have a roughly Gaussian distribution about the centerline of the chamber. One can then write an approximate expression for the electron beam intensity at any place in the beam chamber,

$$I \approx \frac{200,000}{Z^2} \exp\left(\frac{-13r^2}{Z^2}\right) \text{ amperes/cm}^2, \quad (9)$$

$$Z > 10 \text{ cm}$$

where I is the beam intensity (amperes/cm²)
 Z is the distance from the anode (cm)
 r is the distance from the beam-chamber centerline (cm).

The drifting electron beam shows pronounced filamentary structure. The filaments are of interest in themselves, and can be completely removed by a thin scattering foil at the anode.

VII. Conclusions

In recent months we have achieved a very considerable control of and understanding of 3 MeV, 50,000 ampere electron beams. These beams are dominated by their own self forces and show a characteristic tendency to blow up, to pinch, to drift without internal forces, and again to pinch as the gas pressure in the electron beam chamber is increased from 10^{-3} torr to 760 torr.

We have found similar results for electron beams with electron kinetic energy between 1 MeV and 4.6 MeV.

Acknowledgments

I wish to thank the members of the Radiation Physics Group at Physics International Company, without whose initiative and assistance little of this work could have been done.

References

1. J. D. Lawson, Plasma Physics 1, 31-35 (1959).
2. J. D. Lawson, J. Elec. and Cont. 5, 146 (1958).